

Examination of the magnetic properties of NpCo_2

This article has been downloaded from IOPscience. Please scroll down to see the full text article.

1992 J. Phys.: Condens. Matter 4 9423

(<http://iopscience.iop.org/0953-8984/4/47/022>)

View [the table of contents for this issue](#), or go to the [journal homepage](#) for more

Download details:

IP Address: 171.66.16.96

The article was downloaded on 11/05/2010 at 00:55

Please note that [terms and conditions apply](#).

Examination of the magnetic properties of NpCo_2

J P Sanchez†, B Lebecht†, M Wulff§††, G H Landers§, K Tomala†, K
Mattenberger||, O Vogt||, A Blaise†, J Rebizant§, J C Spirlet§ and P J
Brown¶

† Centre d'Etudes Nucléaires, Département de Recherche Fondamentale sur la Matière
Condensée, 85X, F-38041 Grenoble, France

‡ Department of Solid State Physics, Risø National Laboratory, DK-4000 Roskilde,
Denmark

§ Commission of the European Communities, Joint Research Centre, Institute for
Transuranium Elements, Postfach 2340, D-W-7500 Karlsruhe, Germany

|| Laboratorium für Festkörperphysik, Eidgenössische Technische Hochschule, CH-8093
Zürich, Switzerland

¶ Institut Laue-Langevin, 156X, F-38042 Grenoble, France

Received 18 May 1992, in final form 27 July 1992

Abstract. We report a series of measurements on both polycrystalline and single-crystal samples of NpCo_2 in an effort to understand the low-temperature magnetic properties. Previous studies have claimed that NpCo_2 is an antiferromagnet below ~ 13 K. Magnetization and Mössbauer experiments strongly suggest such a transition to an ordered state, although some aspects, such as the relaxation effects seen in Mössbauer spectra far below T_N , are unusual. A variety of neutron experiments, including small-angle scattering and searches along the principal crystallographic directions with a single crystal, have failed to reveal any *direct* evidence for long-range ordering of the Np moments. These measurements do not exclude short-range order or a spin-glass state, although the latter appears to be excluded by the magnetization experiments. At this time we lack an understanding of the low-temperature ground state of NpCo_2 . An account is given of the polarized-neutron experiments in an applied field that give direct evidence of hybridization between Np 5f and Co 3d electrons.

1. Introduction

The actinide Laves phases have been of interest since the early measurements on polycrystalline samples showed that they exhibited a number of unusual properties. In general, the presence or absence of magnetic order can be reconciled with the 'Hill' *ansatz*, which defines a certain distance below which the strong overlap of 5f wavefunctions from neighbouring actinide atoms leads to hybridization of the 5f electrons and a bandwidth too wide to support ordered moments (Hill 1971). If we concentrate on the Np intermetallics, the critical Hill spacing is $d_{\text{Np}} \sim 3.2$ Å. Studies show that for non-magnetic B atoms in the Laves phase structure, which we define as AB_2 with A being an actinide atom, the systems approach itinerant magnetism with low values for the ordered moments as d_{Np} approaches 3.2 Å from a larger value, where pseudo-localized behaviour is found (Aldred *et al* 1974).

†† Present address: European Synchrotron Radiation Facility, BP 220, F-38043 Grenoble, France.

The situation is, of course, more complicated when the B atom is itself magnetic, and the subject of the present investigation is the cubic Laves phase NpCo_2 ($a_0 = 7.043 \text{ \AA}$ at 300 K). In this material the distance between Np atoms is 3.05 \AA ($= a_0\sqrt{3}/4$), so we should anticipate strong hybridization leading to non-magnetic behaviour; however, hybridization also occurs with the unpaired 3d electrons of cobalt B atoms. The result is a Stoner criterion close to one, i.e. the 5f–3d bands become capable of supporting a spontaneous magnetic ordering. Using polycrystalline samples Aldred *et al* (1975) performed systematic studies of the four Np intermetallic compounds NpMn_2 , NpFe_2 , NpCo_2 and NpNi_2 . All compounds were ferromagnetic except for NpCo_2 , which was reported to be antiferromagnetic with $T_N = 15(1) \text{ K}$. However, ordering in NpCo_2 had been proposed earlier (Gal *et al* 1973) to occur at $8.4(2) \text{ K}$. Nevertheless, both groups of investigators (Gal *et al* 1973, Aldred *et al* 1975) showed that the Mössbauer spectra of NpCo_2 exhibit severe line broadening well below the transition temperature. This behaviour was discussed in terms of magnetic relaxation and distribution of hyperfine fields. The latter effect was tentatively ascribed to compositional problems that may exist in NpCo_2 as shown by the neutron data (Aldred *et al* 1975). The influences of slight Co off-stoichiometry on the Mössbauer spectral shape as well as on the lattice parameter was studied by Kalvius *et al* (1985). It was inferred that magnetic order exists for all compositions between $\text{NpCo}_{1.96}$ and $\text{NpCo}_{2.02}$, but the transition temperature was found to decrease with increasing Co content (Gal *et al* 1985). Thus, although the magnetic ordering had not been observed directly by neutrons and certain features of both the magnetization and Mössbauer spectra remained unusual, it was commonly assumed that NpCo_2 did indeed order antiferromagnetically with small moments on both atoms at low temperature.

Our interest in NpCo_2 was renewed some five years ago by two new developments. First, band-structure calculations including orbital-polarization effects suggested that one of the aspects of 5f–3d hybridization could be the reduction of the orbital component μ_L of the magnetic moment in actinide–3d intermetallics (Brooks *et al* 1988, Eriksson *et al* 1986, 1990a, b, 1991). Secondly, at the Institute for Transuranium Elements in Karlsruhe, single crystals of NpCo_2 , UFe_2 and PuFe_2 were produced. The production of these single crystals allowed a series of polarized-neutron experiments on UFe_2 (Wulff *et al* 1989, Lebech *et al* 1989b), PuFe_2 (Wulff *et al* 1988) and NpCo_2 (Wulff *et al* 1990) that accurately measured the spin and orbital contributions to the magnetic moments in ferromagnetically aligned samples. The ratio μ_L/μ_S , where these are the individual orbital and spin components, respectively, was then compared with theoretical predictions. Reviews of this aspect of the work may be found in Lebech *et al* (1991), Eriksson *et al* (1991) and Lander *et al* (1991).

The experiments referred to above on NpCo_2 (Wulff *et al* 1990) were performed on a single crystal in an applied magnetic field of 4.6 T. In such a field the earlier studies (Aldred *et al* 1975) had shown that NpCo_2 was an induced ferromagnet, and the later studies did indeed find $\mu_{\text{Np}} = 0.21(1) \mu_B$ and $\mu_{\text{Co}} = 0.06(1) \mu_B$. This did not answer the question of the zero-field magnetic ordering in NpCo_2 . This paper reports a series of magnetization, Mössbauer and neutron measurements that have been performed over the last three years, some on polycrystalline and some on single-crystal material. Unfortunately, a clear description of the zero-field low-temperature ground state in NpCo_2 remains elusive. Certain measurements point to magnetic ordering, whereas others do not.

2. Magnetization measurements

In this section we shall describe magnetization experiments (i) performed on a SQUID (superconducting quantum interference device) magnetometer on polycrystalline material in the CEN, Grenoble, and (ii) those performed on single crystals with a conventional magnetometer in the ETH, Zürich.

2.1. Magnetization of polycrystalline material

A series of magnetization measurements were performed on a powdered sample of 58 mg encapsulated in a double-walled aluminium container.

First we followed the thermal variation of the magnetization in a 1 T magnetic field from 4.2 K up to ambient temperature. The corresponding inverse molecular susceptibility $1/\chi$ versus T is plotted in figure 1. It shows that a maximum $\chi_M = 4.72(6) \times 10^{-2} \text{ emu mol}^{-1}$ occurs at $T_N = 12.5(5) \text{ K}$. Extrapolation to $T = 0 \text{ K}$ leads to $\chi(0) = 3.7(1) \times 10^{-2} \text{ emu mol}^{-1}$. Above T_N one observes a distinct curvature of the $1/\chi$ versus T curve, which was analysed using a modified Curie-Weiss law:

$$\chi = \chi_0^* + \frac{C^*}{T - \theta_p}$$

from which we deduced $\theta_p = 5 \text{ K}$ and the renormalized $\chi_0 = 0.194 \times 10^{-2} \text{ emu mol}^{-1}$ and $\mu_{\text{eff}} = 1.75 \mu_B$. The overall behaviour of $1/\chi$ versus T is in agreement with Aldred *et al* (1975), but their values of χ_M and T_N are somewhat different to ours ($3.20 \times 10^{-2} \text{ emu mol}^{-1}$ and $15(1) \text{ K}$, respectively), which is not surprising owing to the impurity content and compositional problems of their sample.

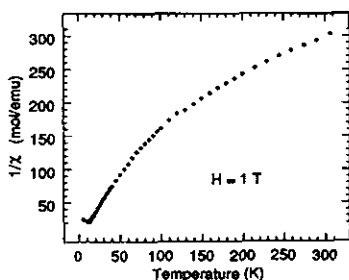


Figure 1. Temperature dependence of the inverse magnetic susceptibility of a polycrystalline sample of NpCo_2 in an applied magnetic field of 1 T.

A series of magnetization versus field measurements up to 5 T show a paramagnetic character above T_N whereas below the apparent ordering temperature an upward curvature of $M(H)$ is observed. No saturation is reached in our maximum field of 5 T. To check for thermomagnetic effects associated with possible spin-glass behaviour (see section 4), $M(H)$ was measured at 6 K after cooling the sample from 100 K in zero-field and in 1 T. No differences were detected. Finally, $\chi(T)$ measurements from 4.2 to 30 K were repeated in different fields to search for a shift of T_N versus H . Some of these curves are displayed in figure 2. They show that χ_M is independent of field, and that T_N is only slightly field-dependent. In 3 T, T_N decreased down to 11.2(2) K; and in 4 T, no temperature maximum is observed but χ shows a plateau from 11 to 4.2 K.

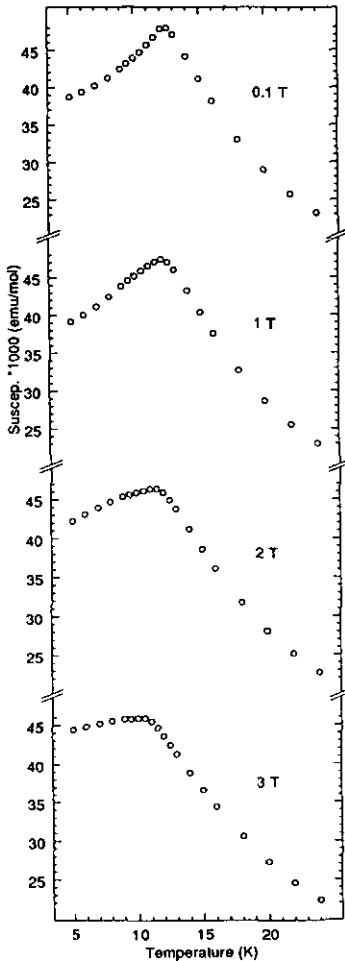


Figure 2. Temperature dependence of the magnetic susceptibility of a polycrystalline sample of NpCo_2 in various applied magnetic fields around the magnetic transition.

2.2. Magnetization of single crystals

The principal results of the single-crystal measurements at 4.2 K are presented in figure 3. The most important point to remark with respect to figure 3 is that it shows that the system exhibits rather little anisotropy. In zero field the state is assumed antiferromagnetic, but a field of ~ 6 T is able to align the moments, which then approach saturation. Although we are accustomed to highly anisotropic magnetic systems in the actinides, this is not always the case, as the example of UFe_2 (Lebech *et al* 1989b) shows. Nevertheless, the lack of anisotropy at low field in NpCo_2 is unusual.

For the purpose of the discussion of the Mössbauer and neutron measurements, we note from figure 3 that at 4.6 T with $\mathbf{H} \parallel \langle 110 \rangle$ the total moment $\mu_{\text{T}} = 0.27(2) \mu_{\text{B}} \text{ mol}^{-1}$; and for $\mathbf{H} \parallel \langle 100 \rangle$ and $H = 6$ T, $\mu_{\text{T}} \sim 0.55 \mu_{\text{B}} \text{ mol}^{-1}$. We can estimate saturation along the easy axis at $\mu_{\text{T}} = 0.60(3) \mu_{\text{B}} \text{ mol}^{-1}$.

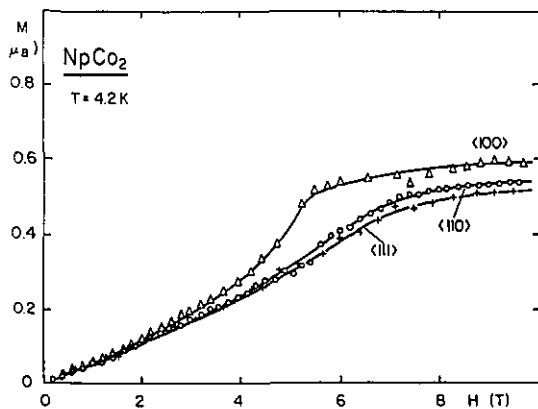


Figure 3. Magnetization of NpCo_2 along the $\langle 100 \rangle$, $\langle 110 \rangle$ and $\langle 111 \rangle$ directions.

3. ^{237}Np Mössbauer experiments

3.1. Mössbauer measurements in the paramagnetic state

3.1.1. *Measurements in zero external field.* At 77 K, i.e. well above the ordering temperature inferred from the magnetization measurements, the Mössbauer spectrum of NpCo_2 consists of a narrow single resonance line with a linewidth of $2.8(2) \text{ mm}^{-1} \text{ s}$ (when the source of ^{241}Am metal is kept at 77 K), as expected for a cubic material. Its isomer shift of $-22.9(2) \text{ mm s}^{-1}$ relative to NpAl_2 suggests that the Np ions are in a tetravalent state. The onset of magnetic ordering at $T_N = 13.0(5) \text{ K}$ is determined from the temperature dependence of the single resonance linewidth, which is almost constant down to the magnetic transition temperature and diverges strongly below. The ordering temperature deduced by Mössbauer spectroscopy is in fair agreement with that deduced from the susceptibility measurements (see section 2.1).

3.1.2. *Measurements under external magnetic field.* The Mössbauer measurements under external magnetic field in the paramagnetic state were undertaken to estimate the local magnetization, and to compare it with the bulk magnetization (Gal *et al* 1989). In the magnetically ordered state the magnetic hyperfine field (H_{hf}) acting at the ^{237}Np nuclei has been shown by Dunlap and Lander (1974) to be proportional to the ordered Np magnetic moment as deduced from the neutron experiments: $H_{\text{hf}}/\mu = 215 \text{ T } \mu_B^{-1}$. This has been interpreted as being an indication that the 5f electrons are well localized. Indeed, if J is a good quantum number, the hyperfine field is proportional to $\langle J_z \rangle$ and thus to the ordered moment ($\mu_{\text{Np}} = g_j \langle J_z \rangle$). However, it appears that the Dunlap-Lander relation is valid even for itinerant and strongly hybridized 5f systems. Because band-structure calculations and neutron experiments on NpCo_2 (Wulff *et al* 1990) indicate a large change in the ratio of orbital to spin moments as compared to localized f-electron behaviour, it was of interest to check further the usefulness of the Dunlap-Lander relation.

The results of the Mössbauer experiment performed at 25 K in a longitudinal (i.e. parallel to the γ -beam) external field (H_{ext}) of 4 T provided by a superconducting magnet are shown in figure 4. The effective magnetic field $H_{\text{eff}} = H_{\text{hf}} + H_{\text{ext}}$ was found to amount to 29 T, thus giving a local magnetization of $0.116 \mu_B/\text{Np}$ using the proportionality constant. This value is slightly smaller than the bulk value of $0.152 \mu_B \text{ mol}^{-1}$ obtained from the magnetization measurements on a polycrystalline

sample. This difference can be attributed to the moment induced at the Co atoms ($\mu_{\text{Co}} \simeq 0.02 \mu_{\text{B}}$). This is a quite reasonable assumption since μ_{Co} with an applied field of 4.6 T was found from polarized-neutron experiments to be $0.06 \mu_{\text{B}}$. Reasonable agreement is therefore found between bulk and local magnetization.

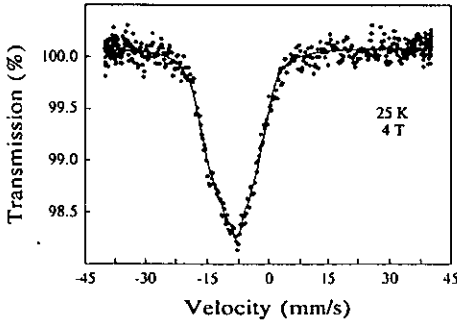


Figure 4. Mössbauer spectrum of NpCo_2 taken in the paramagnetic state at 25 K with an external field of 4 T applied parallel to the γ -ray direction.

3.2. Mössbauer measurement in the ordered state

3.2.1. Measurements in zero external field. Figure 5 shows that broad Mössbauer spectra are observed well below the ordering temperature of $T_N = 13.0(5)$ K. Even at 1.5 K, a single magnetic pattern was unable to reproduce the experimental data. Because our sample is stoichiometric as found by the neutron experiments, one can exclude the earlier explanations (Gal *et al* 1973, Aldred *et al* 1975) and conclude that, at least in our spectra, these effects cannot be due to compositional problems. The unusual temperature dependence of the Mössbauer lineshape indicates either magnetic relaxation effects and/or hyperfine-field (moment) distributions. The Mössbauer spectra at 1.5 and 4.2 K, which are the best resolved, cannot be described by any simple (Lorentzian or Gaussian) static hyperfine-field distribution. Attempts were made also to analyse the spectra assuming a temperature-dependent distribution of hyperfine fields using a histogram method. This procedure may be justified if NpCo_2 orders with a complex spin structure. Although acceptable fits were obtained at 1.5 and 4.2 K (e.g. $\langle H_{\text{hf}} \rangle = 93$ T and $\sigma_{H_{\text{hf}}} = 23$ T at 1.5 K), no coherent picture emerges when one considers the whole temperature range. On the other hand, as demonstrated in figure 6, the Mössbauer data rule out the occurrences of long-period or incommensurate modulated spin structures with a single Fourier component. A consistent description of the spectra taken in the ordered state may be obtained, however, by using a relaxation model in which the hyperfine field (or the magnetic moment) fluctuates around an average value. This model, introduced by Wegener (1965, 1976), and first used to analyse relaxation effects of paramagnetic ions in external fields, was found suitable to treat dynamical effects in the ordered state.

At this stage one should remark that the experimental data cannot be analysed in a self-consistent way using the so-called two-level relaxation model (Nowik and Wickman 1966, Wickman 1966). Indeed, no relaxation effects should be observed at saturation, i.e. when only the ground level is populated. On the other hand, acceptable fits can be obtained only by assuming a linewidth that is temperature-dependent.

Wegener found that, for fast relaxation and a longitudinal fluctuation of the hyperfine field, the lines have Lorentzian shape, but are broadened. For convenience,

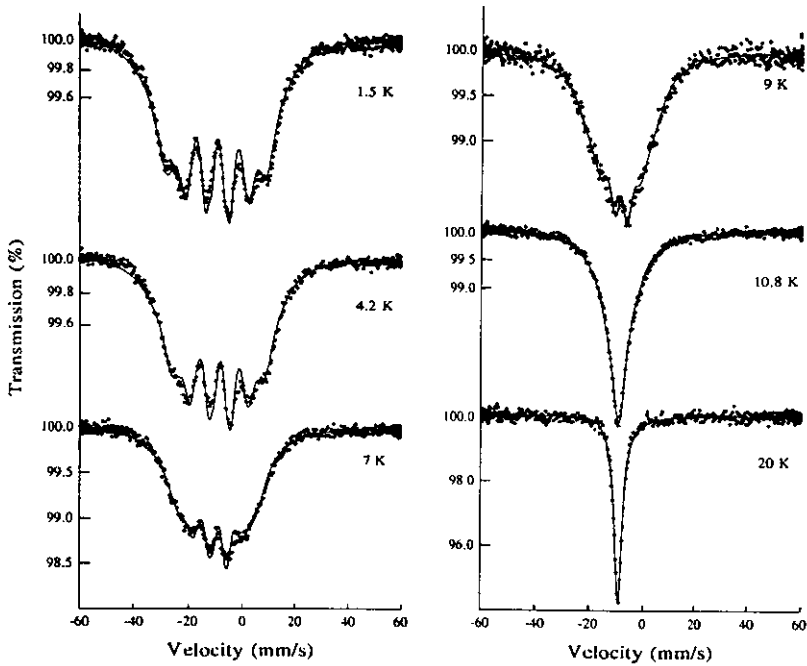


Figure 5. Temperature dependence of the Mössbauer spectra of NpCo_2 . The full curves correspond to fits using the Wegener relaxation model where the intrinsic resonance linewidth is taken as 3.5 mm s^{-1} (see text). The spectrum at 20 K was analysed with a single resonance line fit.

the hyperfine field was expressed as a sum of the time-averaged field $\langle H_{\text{hf}} \rangle$ and the remaining fluctuation part of the field $H_f(t)$:

$$H_{\text{hf}} = \langle H_{\text{hf}} \rangle + H_f(t). \quad (1)$$

The linewidths are then given by

$$W = W_0 + 2\gamma_L(m_e, m_g) \quad (2)$$

where W_0 is the linewidth in the absence of relaxation broadening and

$$\gamma_L(m_e, m_g) = (g_e m_e - g_g m_g)^2 \mu_N^2 \langle H_f^2 \rangle \tau_c \hbar^{-1} \quad (3)$$

where g_e, g_g, m_e and m_g are the nuclear g -factor and the magnetic quantum numbers of the excited and ground states, respectively; τ_c is the longitudinal correlation time.

All spectra in the ordered state were satisfactorily analysed in the frame of this model by constraining the intrinsic linewidth W_0 to 3.5 mm s^{-1} . This choice for W_0 will be justified below. The procedure enabled a least-squares fit to be made of the time-averaged hyperfine magnetic field $\langle H_{\text{hf}} \rangle$, the quadrupole coupling constant $e^2 q_{zz} Q$, the isomer shift δ_{IS} , and the parameter

$$\Delta = f_g^2 \mu_N^2 \langle H_f^2 \rangle \tau_c \hbar^{-1}$$

responsible for the line broadening. The results of this analysis are reported in table 1. Slight improvements of the fits can be achieved when one takes into account shifts of the line positions resulting from the Wegener model, and transverse fluctuations of the hyperfine field (Gabriel 1967). Since this more elaborate model is useless when the spectral resolution is poor (i.e. for $T > 9$ K), and does not introduce any significant change of the values of the relevant hyperfine parameters, it was not considered further. According to table 1, and figure 7, the hyperfine field and the broadening parameter Δ follow a quadratic temperature dependence at least up to $0.7T_N$. At $T = 0$ K the extrapolated average hyperfine field amounts to $\langle H_{\text{hf}}(0) \rangle = 100(1)$ T; this corresponds to an ordered Np magnetic moment of $0.47(1) \mu_B$. The most remarkable point (figure 7) is the non-vanishing fluctuations of the hyperfine field (or magnetic moment) at the lowest temperatures, $\Delta(T = 0) = 1.98(5) \text{ mm s}^{-1}$. Although not yet understood, this behaviour may well be an intrinsic property of this class of highly hybridized materials (Gal et al 1973).

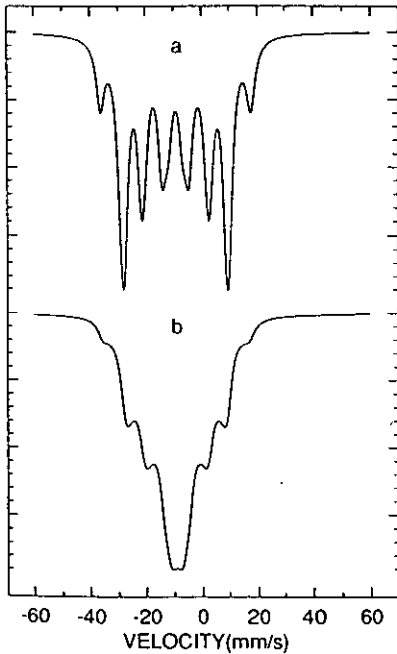


Figure 6. Simulated ^{237}Np Mössbauer spectra for (a) a single magnetic site with $H_{\text{hf}} = 100$ T, $e^2qQ = 0$ and $\delta_{\text{IS}} = -9 \text{ mm s}^{-1}$ and (b) an incommensurate sine-modulated magnetic structure with $H_{\text{hf}}^{\text{max}} = 100$ T, $e^2qQ = 0$ and $\delta_{\text{IS}} = -9 \text{ mm s}^{-1}$. The linewidth W was taken equal to 3.5 mm s^{-1} in both cases.

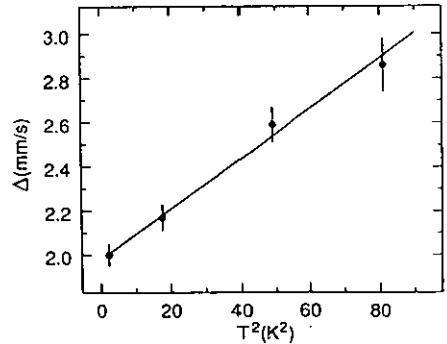


Figure 7. Temperature dependence of the relaxation broadening parameter Δ as obtained from the Wegener model. Notice the non-zero value of Δ at $T = 0$. The straight line is the fit assuming a quadratic temperature dependence.

3.2.2. Measurements under external magnetic field. The measurements have been performed at 4.2 K in longitudinal external fields up to 8 T. Figure 8 shows that the resolution of the magnetically split spectra increases considerably when $H_{\text{ext}} > 5$ T, i.e. in the field-induced ferromagnetic state. The data were analysed using the Wegener

Table 1. ^{237}Np hyperfine parameters of NpCo_2 at different temperatures. The intrinsic linewidth W_0 has been fixed to 3.5 mm s^{-1} (see text). For $E_\gamma = 59.5 \text{ keV}$ gamma transition in ^{237}Np : $1 \text{ mm s}^{-1} = 19.86 \times 10^{-8} \text{ eV} = 48.02 \text{ MHz}$.

T (K)	$\langle H_{\text{eff}} \rangle$ (T)	e^2qQ (mm s^{-1})	δ_{IS} (mm s^{-1}) ^a	Δ (mm s^{-1})
1.5	99.2(8)	1.5(4)	-22.7(2)	2.00(5)
4.2	91.6(1.0)	1.6(6)	-22.3(3)	2.17(6)
7.0	76.2(1.0)	1.8(6)	-22.6(3)	2.59(8)
9.0	58.8(1.4)	1.2(8)	-22.2(5)	2.86(12)
10.8	23.8(8)	1.5 ^b	-22.8(2)	3.86(15)
12.0	13.0(1.8)	1.5 ^b	-22.6(2)	3.78(15)

^a Relative to NpAl_2 .

^b Constrained.

relaxation model with the angle θ between the average effective magnetic field and the γ -beam direction treated as a free parameter. For a saturated ferromagnet θ is expected to tend to zero. The Mössbauer data (table 2) indicate that saturation is not achieved even for $H_{\text{ext}} = 8 \text{ T}$; this is in agreement with the single-crystal magnetization curves (figure 3). However, the main effect of H_{ext} is to reduce the timescale of the fluctuations of the magnetic moment, as shown by the decrease of the broadening parameter Δ with increasing H_{ext} . The spectrum taken at 8 T , showing the best resolution, was fitted using least squares with the intrinsic linewidth W_0 as a variable parameter. W_0 was found to be equal to 3.5 mm s^{-1} . This value has then been fixed in the analysis of all other spectra taken in the ordered state with and without an external field. One should emphasize that, when the data in the ordered state are analyzed with the same Wegener model, the results strongly suggest that the anomalous shape of the Mössbauer spectra is due to dynamical processes.

Table 2. ^{237}Np hyperfine parameters of NpCo_2 at 4.2 K in different external fields.

H_{ext} (T)	$\langle H_{\text{eff}} \rangle$ (T)	e^2qQ (mm s^{-1})	δ_{IS} (mm s^{-1}) ^a	Δ (mm s^{-1})	θ (deg)
0	91.6(1.0)	1.6(6)	-22.3(3)	2.17(6)	random
6	96.8(6)	1.1(4)	-22.5(2)	0.69(4)	26(2)
8	104.3(6)	1.2(4)	-22.6(2)	0.40(3)	19(4)

^a Relative to NpAl_2 .

4. Neutron experiments

As indicated in the abstract to this paper, a number of neutron experiments have been performed. Based on the earlier studies, all experiments, except the studies at high field already reported (Wulff *et al* 1990), were undertaken on the assumption that antiferromagnetic order existed at low temperature. We have found no direct evidence for such a long-range ordered state and outline below the experiments undertaken.

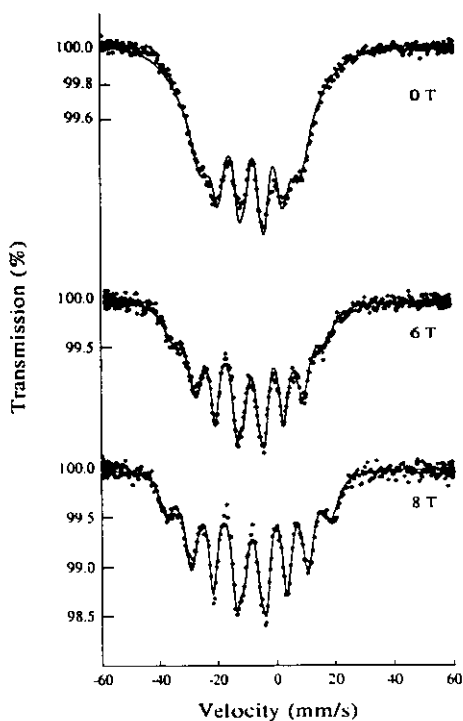


Figure 8. Mössbauer spectra of NpCo_2 at 4.2 K as a function of the external field applied parallel to the γ -ray direction. The full curves correspond to fits using the Wegener relaxation model (see text).

4.1. General characterization of the samples

We shall describe two experiments, both performed at the DR-3 reactor at Risø National Laboratory, in this section. The first is a conventional powder diffraction spectrum taken from a polycrystalline sample (4.32 g) with an incident wavelength of 2.4 Å. This experiment was performed at 50 and 5 K, and no extra peaks corresponding to long-range antiferromagnetic order were found. A refinement of the 13 reflections observed indicated the material to be stoichiometric NpCo_2 . Based on scattering lengths of $b_{\text{Np}} = 1.055$ and $b_{\text{Co}} = 0.249$ (both $\times 10^{-12}$ cm), we believe that any simple antiferromagnetic structure with an ordered moment of $\geq 0.4 \mu_{\text{B}}/\text{Np}$ would have given rise to observable peaks in the 5 K diffraction pattern.

The second characterization experiment performed was aimed at investigating the stoichiometry of the single crystal (both single-crystal and polycrystalline material came from the same batch prepared at Karlsruhe). Since problems of stoichiometry are known to be present in the actinide-cobalt phases (Hrebik and Coles 1977, Zentko et al 1980), and in NpCo_2 in particular (Kalvius et al 1985), we have characterized the single crystal (~ 40 mg) carefully with unpolarized neutrons at a four-circle neutron diffractometer ($\lambda = 1.013$ Å) at Risø. As a result, using the scattering lengths mentioned above and making an absorption correction corresponding to an absorption coefficient of 3.3 cm^{-1} , we conclude that the sample is within 1% of stoichiometry.

4.2. Searching for long-range antiferromagnetic order

A series of three different experiments were performed, in addition to the conventional powder diffraction experiment mentioned in section 4.1, at Risø to

search for complex antiferromagnetic (AF) order. These were undertaken after the analysis of the Mössbauer spectra indicated the possibility of a complex arrangement of moments.

Before discussing the different neutron experiments, we need to consider the absorption of neutrons by ^{237}Np . For the characterization experiments with a single crystal at a neutron wavelength of 1.013 Å (section 4.1 above), and the polarized-beam experiments at the ILL, Grenoble, at wavelengths of 0.8 Å and smaller (Wulff *et al* 1990), absorption is not a serious problem. However, the absorption below 100 meV (≈ 0.9 Å) is proportional to $E^{-1/2}$, or λ , so that it *increases* very substantially at long wavelengths (small energies). Under these conditions a flat sample with the beam passing through perhaps less than 1 mm should be used, but, because of the radioactive and toxic nature of the material, we have performed all experiments on the same samples. The dimensions of the single crystal were $\sim 3 \text{ mm}^3$ with a maximum path length of ~ 2 mm, and the polycrystalline sample was in the form of a loosely packed powder in a vanadium tube of 3 mm internal diameter. Thus the geometries were not ideal for experiments with long-wavelength neutrons.

The first experiments involved the use of small-angle neutron scattering (SANS) of cold neutrons at Risø National Laboratory and the polycrystalline sample mentioned above. Neutrons of mean wavelength of 7 and 14 Å were used and scattering patterns were taken over a range of scattering vector $0.005 < Q < 0.2 \text{ \AA}^{-1}$. (The scattering vector Q , is related to a diffraction peak at a Bragg angle 2θ by $Q = 4\pi\sin\theta/\lambda$.) No difference was observed when the sample temperature was changed from 20 to 5 K.

The second experiment, again using the polycrystalline sample, was to perform careful scans with a cold-source triple-axis spectrometer (5 meV, $\lambda = 4$ Å, neutrons filtered through a cooled Be filter) and cover the Q range of $0.05 < Q < 1.6 \text{ \AA}^{-1}$. A pyrolytic graphite (PG) analyser was used to reduce background. In contrast to the other experiments described, this experiment did give a positive result, albeit rather unexpected. Figure 9 shows the results of subtracting the 5 K from the 20 K data. This result was obtained in two independent runs and shows that over a broad range of Q , centred at $Q \sim 0.09 \text{ \AA}^{-1}$ and with a full-width at half-maximum (FWHM) of 0.06 \AA^{-1} , the scattering is greater at 20 K than at 5 K. This suggests a reduction in the short-range magnetic order below the assumed T_N . This would be reasonable if extra intensity was to appear in sharp Bragg peaks indicating long-range AF order, but we have not found any evidence for such peaks. This experiment also covered the positions of the (1 0 0), (1 1 0) and (1 1 1) Bragg peaks and found no additional scattering at these positions at low temperature. The greater neutron absorption in the SANS experiment than in this one accounts for the fact that the $\sim 15\%$ change in the intensity was not seen in the SANS experiment.

The third experiment was performed with a thermal ($\lambda = 2.4$ Å neutrons) triple-axis spectrometer with the single crystal of NpCo_2 used for the polarized-beam studies. Scans were made along the three principal directions (100), (110) and (111) and no additional peaks were seen at low temperature. In particular, this experiment excluded the simple AF structure proposed by Aldred *et al* (1975), since this structure would give an AF peak at the (2 0 0) position. The latter is forbidden as a nuclear peak in the Laves cubic (C 15) structure. These experiments on a small single crystal with an absorption of $\sim 8 \text{ cm}^{-1}$ are undoubtedly the *most* sensitive we have performed in searching for AF order. However, they have the limitation that, if the structure is complex, the scans may not necessarily intercept the AF peaks, which may occur anywhere in reciprocal space.

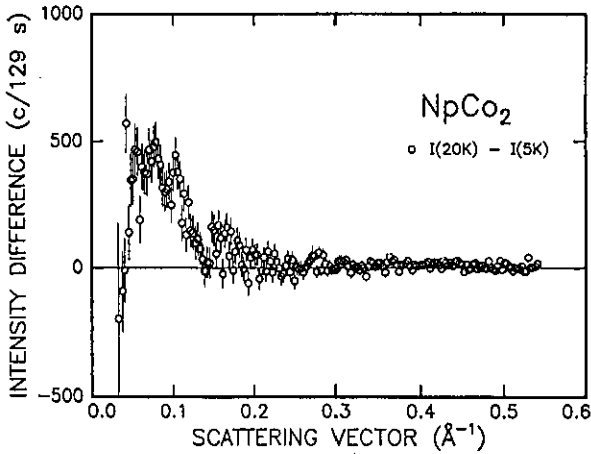


Figure 9. Neutron data showing the difference between the scattering at 20 and 5 K. Data were taken with a cold-source three-axis spectrometer ($E = 5$ meV) set to elastic scattering (Be filter + PG analyser).

In summary, these experiments have not detected any kind of long-range AF order. The one experiment in which there is a difference between the 20 and 5 K data only adds to the confusion as it appears to suggest a decrease of short-range order in cooling from 20 to 5 K, but without the anticipated increase in long-range order.

4.3. Polarized-neutron experiments to determine $f(Q)$

These experiments were performed on the single crystal mentioned above at the D3 polarized-neutron diffractometer installed at the high-flux reactor, ILL, Grenoble. Part of the results have been reported in Wulff *et al* (1990). However, for completeness, we shall summarize all the results here but omit the results of theoretical calculations, which were reported briefly in Wulff *et al* (1990) and in more detail in Eriksson *et al* (1991).

Figure 10 shows the Np form factor deduced from experiments with an applied field of 4.6 T. A neutron wavelength of 0.843 Å, with an appropriate filter to reduce the $\lambda/2$ components, was used to collect most of the data. Some data were also collected at 0.71 Å. No evidence for extinction was found, but this is not surprising in view of the appreciable absorption involved ($\mu = 2.7$ cm⁻¹ at this energy). The field was applied in a direction very close to [4 3 0], which is 8° from a $\langle 110 \rangle$ direction. The induced moment was found to align along the field direction, as expected from the small anisotropy shown at these field strengths in figure 3.

The polarized-beam method is fully described in a number of recent studies on actinide intermetallics, most notably that on PuFe₂ (Wulff *et al* 1988) and on URhAl (Paixão *et al* 1992). The method measures the ratio of the magnetic M to nuclear N structure factors. Since our earlier studies with a four-circle diffractometer on the same crystal of NpCo₂ verified the N values, the values of M may be derived. The details are presented in table 3. Three reflections in the set measured have a contribution from Co only in the Laves phase structure. These are plotted in figure 10. Their decrease with $\sin \theta/\lambda$ is consistent with the form factor of elemental Co and extrapolates to 0.06(1) μ_B at the cobalt site. Most structure factors have a contribution from Co, which is subtracted assuming the moment above and a standard form factor. The remaining contribution is $(\mu f)_{Np}$ and is plotted in the figure. In five cases (full circles in the figure) the structure factors are from Np only.

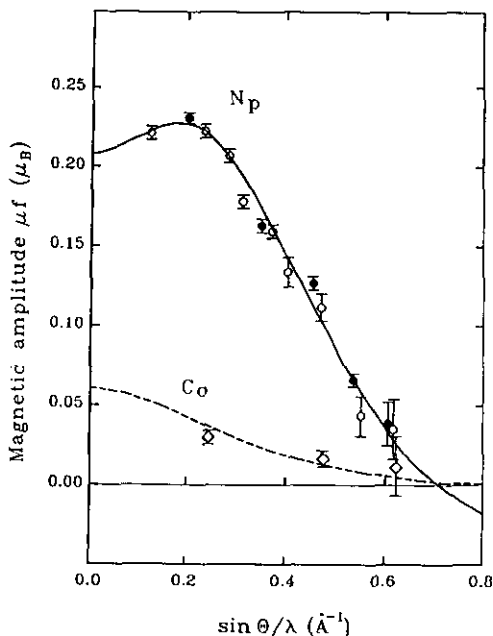


Figure 10. Magnetic amplitudes $(\mu f)_{\text{Np}}$ and $(\mu f)_{\text{Co}}$ in NpCo_2 in an applied magnetic field of 4.6 T. The open diamonds correspond to Co-only reflections (type *d* in table 3). The full circles correspond to reflections with a contribution from Np only (type *b* in table 3). The reflections denoted with open circles contain a contribution from both atoms (see table 3), so it is necessary to correct for $(\mu f)_{\text{Co}}$ before plotting the $(\mu f)_{\text{Np}}$ value. The broken curve is the form factor of elemental Co; the full curve is described in the text.

We fit the $(\mu f)_{\text{Np}}$ by recalling that, in the dipole approximation (Marshall and Lovesey 1971)

$$(\mu f)_{\text{N}} = \mu_{\text{S}} \langle j_0 \rangle + \mu_{\text{L}} (\langle j_0 \rangle + \langle j_2 \rangle)$$

where μ_{S} and μ_{L} are the spin and orbital moments on the Np site and $\langle j_i \rangle$ are Bessel transforms (Desclaux and Freeman 1978) of the single-electron charge-density distribution $U_{5f}^2(\tau)$. The $\langle j_i \rangle$ functions are $Q (= 4\pi \sin \theta / \lambda)$ dependent. The full curve, which is an excellent fit to the data, uses

$$\mu_{\text{Np}} = 0.21(1)\mu_{\text{B}}$$

$$\mu_{\text{S}} = -0.6(1)\mu_{\text{B}}$$

$$\mu_{\text{L}} = 0.8(1)\mu_{\text{B}}$$

Normally the dipole approximation is not valid for $\sin \theta / \lambda \simeq 0.5 \text{ \AA}^{-1}$ so that we also introduce a term in $\langle j_4 \rangle$. This procedure leads to a significant reduction in χ^2 but does not substantially change the derived values of the moments.

These fits are unable to distinguish between $\text{Np}^{3+} 5f^4$ or $\text{Np}^{4+} 5f^3$ configurations, primarily because the $\langle j_i \rangle$ functions for Np^{3+} and Np^{4+} are very similar. Nor do we know how close the real $\langle j_i \rangle$ functions in the solid NpCo_2 are to the tabulated free-ion values. Normally, an excellent test of the ionicity is the ratio $-\mu_{\text{L}} / \mu_{\text{S}}$ (see Lebech *et al* 1991, Lander *et al* 1991). For NpCo_2 we find $-\mu_{\text{L}} / \mu_{\text{S}} = 1.3(2)$ whereas for f^3 this should be 2.6 and for f^4 should be 1.9. As we have discussed earlier (Wulff *et al* 1990), the low value of $-\mu_{\text{L}} / \mu_{\text{S}}$ is due to the reduction of μ_{L} that arises from strong hybridization between the Np 5f and Co 3d electrons. Thus, it is impossible from the neutron results to assign a specific ionicity to the Np site, but the projected 5f density in the band-structure calculations suggests a configuration near $5f^4$ (Eriksson *et al* 1991). The Mössbauer isomer-shift measurements (section 3) suggest a $5f^3$ configuration.

Table 3. Values determined at 5 K and an applied magnetic field of 4.6 T by polarized neutrons for single-crystal NpCo₂. N is the nuclear structure factor, determined by using scattering lengths $b_{\text{Np}} = 1.055$ and $b_{\text{Co}} = 0.249$ (both $\times 10^{-12}$ cm) for Np and Co, respectively. The M values refer to eight formula units in the unit cell. The ratio $\gamma = M/N$, where M is the magnetic structure, is determined experimentally, from which M is deduced. The Co contributions are derived by assuming a moment of $\mu_{\text{Co}} = 0.06 \mu_{\text{B}}$ and the elemental Co form factor. The N values per formula unit are $a = b_{\text{Co}} - b_{\text{Np}}/\sqrt{2}$, $b = b_{\text{Np}}$, $c = b_{\text{Co}} + b_{\text{Np}}/\sqrt{2}$, $d = 2b_{\text{Co}}$, $e = 2b_{\text{Co}} - b_{\text{Np}}$, $f = 2b_{\text{Co}} + b_{\text{Np}}$. (The conventions here are the same as in Wulff *et al* (1988).) Standard deviations refer to the least significant digit.

hkl	$\sin \theta/\lambda$ (\AA^{-1})	N	$ M $	$(\mu f)_{\text{Np}}$ (μ_{B})	$(\mu f)_{\text{Co}}$ (μ_{B})
111	0.123	a	0.847(10)	0.224(6)	
220	0.201	b	1.880(20)	0.235(3)	
311	0.236	c	1.56(3)	0.225(7)	
222	0.247	d	0.50(3)	—	0.032(2)
400	0.285	e	1.18(3)	0.211(7)	
331	0.310	a	0.79(2)	0.182(6)	
422	0.349	b	1.31(4)	0.166(5)	
333	0.370	c	1.00(4)	0.163(6)	
511	0.370	c	1.13(4)		
440	0.403	f	1.35(7)	0.137(11)	
620	0.405	b	1.01(5)	0.130(6)	
533	0.467	c	0.73(4)	0.114(9)	
622	0.472	d	0.31(8)	—	0.019(5)
642	0.532	b	0.53(5)	0.068(6)	
533	0.547	c	0.30(7)	0.05(1)	
731	0.547	c	0.33(9)		
800	0.569	f	0.98(12)	0.115(16)	
660	0.604	b	0.38(20)	0.040(15)	
822	0.604	b	0.23(12)		
555	0.616	c	0.35(17)	0.041(19)	
751	0.616	c	0.16(10)		
662	0.620	d	0.24(30)		0.015(20)

The total moment per mole is therefore $\mu_{\text{Np}} + 2\mu_{\text{Co}} = 0.33(3) \mu_{\text{B}}$. The magnetization measurements give $0.27(2) \mu_{\text{B}}$ at this field, so that the conduction-electron polarization is $-0.06(4) \mu_{\text{B}}$. This is a quite reasonable value, with the usual sign, in such an actinide intermetallic (see Lebech *et al* 1989b).

4.4. Neutron examination of maximum in susceptibility

In addition to examining the induced form factor at 4.2 K and $H = 4.6$ T (section 4.3, figure 10) we have also examined the (2 2 0) magnetic structure factor as a function of applied field H and temperature T . When these measurements were performed we did not have the susceptibility measurements reported in section 2, and were thus interested to establish whether the maximum in χ reported by Aldred *et al* (1975) also existed in our material. We recall from table 3 that the (2 2 0) reflection arises from Np contributions only.

The results of these investigations are shown in figure 11. This quantity (γ/H) is directly proportional to susceptibility, and figure 11 shows a remarkable similarity to the bulk susceptibility data shown in figure 2. We can make a number of remarks with respect to this figure. First, the maximum is clearly associated with the Np moments and is very prominent at low fields. Secondly, as in figure 2, the height of the maximum is nearly independent of field, and the maximum decreases slightly in temperature with increasing field. Thirdly, at high fields the susceptibility exhibits more of a plateau than a maximum.

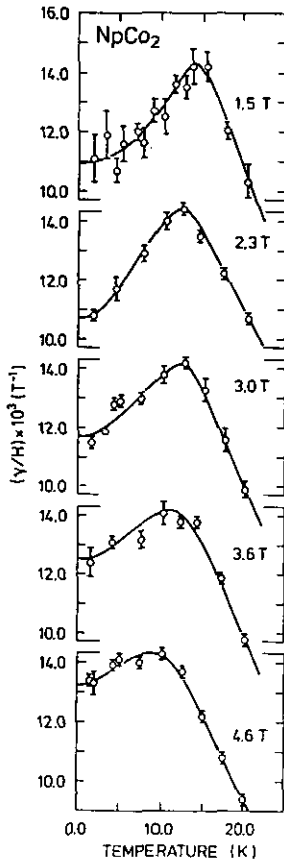


Figure 11. The quantity $\gamma = M/N$, where M and N are the magnetic and nuclear structure factors, respectively, of the (2 2 0) reflection normalized by the applied field and plotted as a function of temperature for various applied fields. The curves are spline fits through the points. The ordinate is directly proportional to susceptibility (see text).

5. Discussion

Certain aspects of NpCo_2 are now understood. From the viewpoint of electronic structure we know that the 5f from neptunium and 3d electrons from cobalt are strongly hybridized, and this process results in a decrease of the orbital magnetic moment compared to the spin 5f moment. This was first noted by Wulff *et al* (1990), and a more detailed discussion of the actinide intermetallics has been given by Lebech *et al* (1991), Eriksson *et al* (1991) and Lander *et al* (1991).

However, the main thrust of the majority of the measurements in this paper has been to elucidate the zero-field ground state in NpCo_2 . We have not succeeded in this endeavour. Magnetization (section 2) and Mössbauer (section 3) measurements appear to point unambiguously to the development of long-range order in NpCo_2 at ~ 13 K. In this regard the measurements are consistent with earlier work by Gal *et al* (1973) and Aldred *et al* (1975). The Mössbauer hyperfine field of 99.2 T at 1.5 K implies a magnetic moment of $0.46 \mu_{\text{B}}/\text{Np}$ atom (Dunlap and Lander 1974). If we include the $\sim 0.1 \mu_{\text{B}}$ anticipated at saturation on the Co atom and the $\sim -0.06 \mu_{\text{B}}$ of conduction-electron polarization we obtain

$$\mu = \mu_{\text{Np}} + 2\mu_{\text{Co}} + \mu_{\text{cep}} \sim 0.46 + 0.2 - 0.06 \sim 0.60 \mu_{\text{B}} \text{ mol}^{-1}.$$

This is clearly in excellent agreement with the high-field magnetization experiments of section 2.1 (figure 3). The magnetization effects show no unusual field-dependent effects, except the increasing susceptibility below 12 K up to ~ 6 T, and thus we can exclude a conventional spin-glass state. A summary of the various moment values discussed in the text is provided in table 4.

Table 4. Summary of the moment values discussed in the text and deduced from the various techniques. The induced moments at $H = 4.6$ T are given, together with saturated moments for magnetization and Mössbauer techniques. μ_{T} is the total moment per mole, μ_{Np} that on neptunium, μ_{Co} that on cobalt.

		Moments (μ_{B})	
		$H = 4.6$ T	Saturation
Magnetization			
$H \parallel (110)$	μ_{T}	0.27(2)	
Easy axis	μ_{T}		0.60(3)
Mössbauer	μ_{Np}		0.46(1)
Neutrons	μ_{Np}	0.21(1)	
$H \parallel (110)$	μ_{Co}	0.06(1)	

The Mössbauer spectra show strong relaxation effects (see section 3). Severe line broadening occurs still at 1.5 K, at which temperature relaxation effects would be expected to be negligible. At the lowest temperatures (figure 5) the spectra is complex and cannot be fitted easily with a complex magnetic order (see figure 6). A more likely hypothesis is that important relaxation effects occur. A fit with the Wegener model is satisfactory. It leads to dependences of the mean hyperfine field (H_{hf}) and the relaxation broadening parameter Δ that are quadratic with temperature. Surprisingly, Δ is still relatively large (2 mm s^{-1}) at the lowest temperature of 1.6 K. The relaxational effects are reduced with increasing applied field (figure 8) but not eliminated even at 8 T.

The search for direct evidence of AF order in the neutron diffraction patterns is the subject of section 4. No such direct evidence has been found. We are particularly surprised that neither the SANS experiments (section 4.2) nor those with a three-axis spectrometer on both polycrystalline and single-crystal samples (section 4.2) were successful. The use of the SANS technique was motivated by the suggestion that some long-range spiral or longitudinal wave-like AF structure might be present, as in FeGe and MnSi, for example (Lebech *et al* 1989a). Despite small moments and very long AF periodicities (repeat lengths of $\sim 180 \text{ \AA}$), these structures can be seen by the

SANS technique because at low scattering angles the AF peaks are much enhanced by the Lorentz and powder factor $L = [\sin \theta \sin(2\theta)]^{-1}$, where 2θ is the Bragg angle. All these various attempts are described in section 4. We cannot, of course, completely exclude some complex type of AF order. The absorption of both Np and Co is large at low neutron energies and this inevitably reduces the sensitivity of the searches performed. The neutron measurements are, however, consistent with either the formation of a spin glass or some other type of short-range correlations at ~ 13 K. Such correlations, as found for example in the superconducting cuprates (Shirane *et al* 1989, Cheong *et al* 1991), would give rise to weak broad peaks in the neutron patterns that might easily have been missed in the neutron studies performed so far on NpCo_2 .

Acknowledgments

We would like to thank the Radioprotection Staff at both Risø and Grenoble for their cooperation in the studies of this transuranium sample. We thank C Rijkeboer for his help with the crystal growth, E Bednarczyk for help with the encapsulation, and M Brooks for useful discussions. The small-angle scattering experiment was done in collaboration with K Mortensen and J Skov Pedersen and their expertise and help is much appreciated.

References

- Aldred A T, Dunlap B D, Lam D J, Lander G H, Mueller M H and Nowik I 1975 *Phys. Rev. B* **11** 530
Aldred A T, Dunlap B D, Lam D J and Nowik I 1974 *Phys. Rev. B* **10** 1011
Brooks M S S, Eriksson O, Johansson B, Franse J J M and Frings P H 1988 *J. Phys. F: Met. Phys.* **18** L33
Cheong S W, Aeppli G, Mason T E, Mook H, Hayden S M, Canfield P C, Fisk Z, Clausen K N and Martinez J L 1991 *Phys. Rev. Lett.* **67** 1971
Desclaux J P and Freeman A J 1978 *J. Magn. Magn. Mater.* **8** 119
Dunlap B D and Lander G H 1974 *Phys. Rev. Lett.* **33** 1046
Eriksson O, Brooks M S S and Johansson B 1990a *Phys. Rev. B* **41** 9087
Eriksson O, Brooks M S S, Johansson B, Albers R C and Boring A M 1991 *J. Appl. Phys.* **69** 5897
Eriksson O, Johansson B, Albers R C, Boring A M and Brooks M S S 1990b *Phys. Rev. B* **42** 2707
Eriksson O, Johansson B, Skriver H L and Brooks M S S 1986 *Physica B* **144** 32
Gabriel H 1967 *Phys. Status Solidi* **23** 195–205
Gal J, Fredo S, Potzel W, Asch L and Kalvius G M 1985 unpublished results
Gal J, Hadari Z, Atzomy U, Bauminger E R, Nowik I and Ofer S 1973 *Phys. Rev. B* **8** 1901
Gal J, Litterst F J, Potzel W, Moser J, Potzel U, Fredo S, Tápuchi S, Shani G, Jové J, Cousson A, Pagès M and Kalvius G M 1989 *Phys. Rev.* **63** 2413–16
Hill H 1971 *Plutonium 1970 and Other Actinides* ed W N Miner (New York: AIME) p 29
Hrebik J and Coles B R 1977 *Physica B* **86–88** 169
Kalvius G M, Potzel W, Moser J, Litterst F J, Asch L, Zankert J, Potzel U, Kratzer A, Wunsch M, Gal J, Fredo S, Dayan D, Dariel M P, Boge M, Chappert J, Spirtet J C, Benedict U and Dunlap B D 1985 *Physica B* **130** 393
Lander G H, Brooks M S S and Johansson B 1991 *Phys. Rev. B* **43** 13, 672
Lebech B, Bernhard J and Freltoft T 1989a *J. Phys.: Condens. Matter* **1** 6105
Lebech B, Wulff M and Lander G H 1991 *J. Appl. Phys.* **69** 5891
Lebech B, Wulff M, Lander G H, Rebizant J, Spirtet J C and Delapalme A 1989b *J. Phys.: Condens. Matter* **1** 10229
Marshall W and Lovesey S W 1971 *Theory of Thermal Neutron Scattering* (London: Oxford University Press) p 152

- Nowik I and Wickman 1966 *Phys. Rev. Lett.* **17** 949
- Paixão J A, Lander G H, Brown P J, Nakotte H, de Boer F R and Brück E 1992 *J. Phys.: Condens. Matter* **4** 829
- Shirane G, Birgeneau R J, Endoh Y, Gehring P, Kastner M A, Kitazawa K, Kojima H, Tanaka I, Thurston T R and Yamada K 1989 *Phys. Rev. Lett.* **63** 330
- Wegener H 1965 *Z. Phys.* **186** 498-511
- 1976 *Proc. Int. Conf. on Mössbauer Spectroscopy (Cracow, Poland)* vol 2, ed A Z Hryniewicz and J Sawicki (Krakow: Akademia Gorniczo-Hutnicza Im. S. Staszika W. Krakowie) p 257
- Wickman H H 1966 *Mössbauer Effect Methodology* vol 2, ed Groverman (New York: Plenum) p 39
- Wulff M, Eriksson O, Johansson B, Lebech B, Brooks M S S, Lander G H, Rebizant J, Spirlet J C and Brown P J 1990 *Europhys. Lett.* **11** 269
- Wulff M, Lander G H, Lebech B and Delapalme A 1989 *Phys. Rev. B* **39** 4719
- Wulff M, Lander G H, Rebizant J, Spirlet J C, Lebech B, Broholm C and Brown P J 1988 *Phys. Rev. B* **37** 5577
- Zentko A, Hrebik J, Sternberk J and Turan J 1980 *Physica B* **102** 269